Selective DNA-Mediated Assembly of Gold Nanoparticles on Electroded Substrates

K. E. Sapsford,[†,‡,▽] D. Park,[§] E. R. Goldman,[‡] E. E. Foos,[||] S. A. Trammell,[‡] D. A. Lowy,[⊥] and M. G. Ancona*[,§]

George Mason University, 10910 University Boulevard, Manassas, Virginia 20110, Naval Research Laboratory, Center for Bio/Molecular Science and Engineering, Electronics Science and Technology Division, and Chemistry Division, Naval Research Laboratory, Washington, D.C. 20375, Nova Research, Inc., Alexandria, Virginia 22308

Received February 28, 2008. Revised Manuscript Received June 18, 2008

Motivated by the technological possibilities of electronics and sensors based on gold nanoparticles (Au NPs), we investigate the selective assembly of such NPs on electrodes via DNA hybridization. Protocols are demonstrated for maximizing selectivity and coverage using 15mers as the active binding agents. Detailed studies of the dependences on time, ionic strength, and temperature are used to understand the underlying mechanisms and their limits. Under optimized conditions, coverage of Au NPs on Au electrodes patterned on silicon dioxide (SiO_2) substrates was found to be ∼25−35%. In all cases, Au NPs functionalized with non-complementary DNA show no attachment and essentially no nonspecific adsorption is observed by any Au NPs on the SiO_2 surfaces of the patterned substrates. DNA-guided assembly of multilayers of NPs was also demonstrated and, as expected, found to further increase the coverage, with three deposition cycles resulting in a surface coverage of approximately 60%.

Introduction

Gold nanoparticles (Au NPs) have generated significant interest because of the ease with which they can be synthesized, and because of the technological possibilities they offer for sensors and for electronics.[1] As is often the case in nanotechnology, the sensor applications are the most developed with the metal−insulator−metal-ensemble (MIME) chemical vapor sensor approach being well-known.[2] These sensors, which depend on the exponential characteristics of interparticle transport, are typically formed on SiO_2 surfaces with patterned gold electrodes.[3] The uses of Au NPs for electronics are much more speculative with their promise engendered primarily by the fact that, due to their ultrasmall size, their electrical properties are dominated by single-electron charging effects.[4] This in turn suggests the possibility of an electronics technology based on single-electron-transistors that would be on the scale of a few nanometers and that would operate at room temperature. Much like the MIME sensors (though at a much greater scale of integration), these nanoparticle-based switches would also have to be positioned and interconnected on patterned substrates. The focus of the present paper is on this latter task, and in particular on DNA-based methods for selectively positioning nanoparticles on patterned electronic substrates.

Although practical applications have yet to be realized, the notion that one might use the Watson−Crick base-pairing of DNA as a means for ultrahigh-precision engineering is well-known.[5,6] The idea is to use the highly specific hybridization chemistry that occurs between specific sequences of complementary single-stranded DNA (ssDNA) to guide a sophisticated chemical self-assembly of components into complex engineered systems such as electronic circuits. The present paper explores a much more primitive version of such self-assembly, where we demonstrate protocols for the selective and efficient DNA-guided attachment of 12nm Au NPs to Cr/Au electrodes patterned onto SiO_2 surfaces. To functionalize the electrodes with Au NPs, single-stranded (ss) DNA templates are first immobilized onto the Cr/Au electrodes via gold-thiol-driven assembly. This is followed by hybridization of Au NPs functionalized with complementary ssDNA. The efficiency of the assembly was monitored by SEM. Various reaction conditions were investigated in order to maximize the density of Au NPs immobilized on the electrode surfaces. These studies included varying the NaCl concentration, investigating the addition of surfactant, and changing the DNA-to-thiol spacer used when depositing the ssDNA templates. Also studied were the effects of temperature, NaCl concentration and surfactant on the hybridization of the DNA functionalized Au NPs to the templates. In addition, we investigated the DNA-driven assembly of multilayers of Au NPs. All of these experiments and the effects of the various parameters on the attachment of Au NPs to electronic substrates are described.

Materials and Methods

Materials. All purchased materials were used as received unless otherwise stated. Sodium citrate, hydrogen tetrachloroaurate gold ($HAuCl_4$), DL-dithiothreitol (DTT), sodium dodecyl sulfate (SDS), phosphate buffer (PB), sodium chloride (NaCl), Tris-EDTA buffer (TE), and Tween 20 were all purchased from Sigma-Aldrich. The Zeba spin columns used in purification procedures were obtained

* To whom correspondence should be addressed. E-mail: ancona@estd.nrl.navy.mil.

† George Mason University.

‡ Center for Bio/Molecular Science and Engineering, Naval Research Laboratory.

§ Electronics Scienc and Technology Division, Naval Research Laboratory.

|| Chemistry Division, Naval Research Laboratory.

⊥ Nova Research, Inc.

▽ Present address: U.S. Food and Drug Administration, CDRH/OSEL/DB, Building 64 HFZ-110, 10903 New Hampshire Ave, Silver Spring, MD 20993.

(1) Brust, M.; Walker, M.; Bethell, D.; Schiffrin, D. J.; Whyman, R. *J. Chem. Soc. Chem. Commun.* **1994**, *7*, 801.

(2) Wohltjen, H.; Snow, A. W. *Anal. Chem.* **1998**, *10*, 947.

(3) Ancona, M. G.; Snow, A. W.; Foos, E. E.; Kruppa, W.; Bass, R. *IEEE Sensors J.* **2006**, *6*, 1403.

(4) Andres, R. P.; Bein, T.; Dorogi, M.; Feng, S.; Henderson, J. I.; Kubiak, C. P.; Mahoney, W.; Osifchin, R.; Reifenberger, R. *Science* **1996**, *272*, 1323.

(5) Seeman, N. *Mol. Biotechnol.* **2007**, *37*, 246.

(6) Jhaveri, S. D.; Foos, E. E.; Lowy, D. A.; Chang, E. L.; Snow, A. W.; Ancona, M. G. *Nano Lett.* **2004**, *4*, 737.

10.1021/la800640u CCC: $40.75
Published on Web 08/15/2008

Table 1. IDT Purchased ssDNA Sequences and Select Physical Properties

ssDNA sequence name	ssDNA sequence	T_m °C	ext. coefficient 260 nm L/(mol·cm)
No Spacer[a]			
NCseq/15mer	5′-/5ThiolMC6-D/ACT TCG GAC GCA TAC-3′	48.2	143 200
Cseq	5′-/5ThiolMC6-D/GTA TGC GTC CGA AGT-3′	48.2	146 700
CseqFAM	5′-/5ThiolMC6-D/GTA TGC GTC CGA AGT/36-FAM/-3′	48.2	156 700
Poly T Spacer			
25mer	5′-/5ThiolMC6-D/TTT TTT TTT TAC TTC GGA CGC ATA C-3′	52.9	224 100
Fluor25mer	5′-/5ThiolMC6-D/TTT TTT TTT TAC TTC GGA CGC ATA C/36-FAM/-3′	52.9	245 100
35mer	5′-/5ThiolMC6-D/TTT TTT TTT TTT TTT TTT TTA CTT CGG ACG CAT AC-3′	56.1	305 100
PEG Spacer			
Peg-15mer	5′-/5ThiolMC6-D//iSp9/ACT TCG GAC GCA TAC-3′	48.2	143 200

[a] Note: Other than Cseq all the ssDNA used in these studies have the same 15mer sequence as NCseq, which is complementary to Cseq.

from Pierce. The particular ssDNAs used to affect the assemblies in this work are summarized in Table 1 along with some of their physical properties. These molecules, all purchased in HPLC-purified form from Integrated DNA Technologies, consisted of up to five distinct parts which in order are: (i) a thiol linker for attaching to gold, (ii) a 6 methylene unit spacer, (iii) an optional ssDNA spacer, (iv) the oligomer whose specific sequence is used to guide the assembly, and (v) an optional fluorescent tag. The chosen oligomer sequences were selected to avoid self-loops, partial hybridizations and unwanted cross-linking. As bought, the thiol linkers were protected with a disulfide linkage that, prior to use, had to be reduced to free thiols as described below.

Preparation of 12 nm Au NPs. Au NPs were prepared using a slightly modified literature procedure.[7] Briefly, 25 mL of a 1 mM solution of $HAuCl_4$ in triply distilled H_2O was brought to a boil with rapid stirring, and 2.5 mL of a 38.8 mM solution of sodium citrate in triply distilled H_2O was added quickly. Then the solution was boiled for 15 min during which time the color progressed from light yellow to a deep red. Next, the solution was allowed to cool to room temperature while stirring. It was transferred to a capped vial and stored at 9 °C until use. The concentration of the final 12 nm Au NPs was determined using UV−visible spectroscopy by measuring the absorbance at 520 nm (surface plasmon peak) and an approximate extinction coefficient of 1×10^8L/(mol·cm).[8] Typically, the as-prepared concentrations were ∼30−35 nM.

Deprotection of ssDNA. Deprotection of the 5ThiolMC6-D disulfide group on the as-bought ssDNA sequences was typically performed just prior to use. Frozen 20 nmol ssDNA aliquots were rehydrated in 50 μL deionized water (MilliQ, 18.2 MΩ·cm), and 5 μL of 1 M DTT in MilliQ water added, and then incubated at RT for 45−60 min. Following incubation, 200 μL MilliQ water was added to increase the final reaction volume to 250 μL. Excess DTT was then removed using Zeba spin columns, and a benchtop centrifuge (2 min 1000*g* spins), following the manufacturer's instructions. Briefly, the Zeba spin columns were first washed with 4 × 1 mL aliquots of MilliQ water, the ssDNA/DTT solution was then loaded onto the column and spun at 1000*g* for 2 min. The purified and deprotected ssDNA that elutes from the column was characterized by UV−visible absorption spectroscopy, and stored in a clean Eppendorf tube.

Au NP Functionalization With ssDNA and Subsequent Purification and Characterization. The procedure used to attach ssDNA to the surface of the Au NPs was originally developed and optimized by Hurst and co-workers.[9] Details of this and the methods used to purify and characterize the resulting ssDNA-Au NPs are provided in the Supporting Information.[9,10]

Preparation of Electroded Substrates. The substrates used were Si wafers thermally oxidized to provide a 50 nm thick insulating SiO_2 layer with very low leakage current. To define the electrodes, a standard lift-off procedure was employed in which a PMMA resist was deposited and defined by e-beam. A 2 nm Cr adhesion layer followed by a 50 nm Au layer were then evaporated (using an e-beam Veeco system, Veeco Instruments, Inc., Woodbury, NY). Stripping off the resist left the desired electrodes, which consisted of micron-scale features in a variety of test patterns. As a last step, these substrates were diced into ∼5 mm × 5 mm square test pieces for use in the experiment; hereafter these test pieces are referred to as "SiO_2/Au substrates". For a few experiments, alternative test pieces entirely covered with evaporated Au were used; these are referred to below as "Au substrates".

Functionalization of Electroded Substrates With ssDNA Template. The SiO_2/Au and Au substrates were cleaned by quick immersion in chloroform, and then allowed to air-dry before being cleaned in a UV-ozone cleaner (Samco Model UV-1, SAMCO International, Inc., Sunnyvale, CA), with a 20 min exposure to the UV-ozone at 150 °C at a flow-rate of 0.5 L/min, followed by a 2 min nitrogen purge. Following the UV-ozone cleaning, the substrates were immediately immersed in a 2 μM solution (1.5 mL) of the freshly cleaved and purified ssDNA template in 1xTE + 2 M NaCl + 0.05% Tween 20 for a minimum of 12 h at RT. The Tween 20 is a widely used surfactant, which was found to be very effective in preventing nonspecific binding of the ssDNA template to the SiO_2 exposed regions of the Au/SiO_2 substrates in the presence of NaCl (data not shown). Various ssDNA templates were employed in this study including 15mer, 25mer, 35mer and Peg-15mer, all complementary to the Cseq ssDNA sequence, and various buffer conditions were investigated, as described in the Results and Discussion Section below.

DTT Assay on Au Substrates. To quantify the number of ssDNAs attached per area of Au substrates as a function of NaCl concentration, the substrates were cleaned and immediately immersed in a 2 μM solution of freshly deprotected and purified Fluor25mer template in 1xTE + 0.05% Tween 20 with a range of concentrations of NaCl. All substrates were left in contact with the deposition solution for a minimum of 12 h, and then were thoroughly rinsed with MilliQ water. After drying, the substrates were transferred into separate small glass vials and 100 μL of MilliQ water was added followed by 100 μL of 1 M DTT in 0.18 M PB pH 8.0−8.5. The vials were left in the dark at RT overnight. As before, using known concentrations of the Fluor25mer to create a dose−response in the 1 M DTT in 0.18 M PB pH 8.0−8.5, the fluorescence intensity of the solution in the vials was measured using a SPEX Fluorolog-3 spectrofluorometer (HORIBA Jobin Yvon Inc., Edison, NJ) and the concentration of the Fluor25mer in the samples determined. The geometric surface area (excluding surface roughness) of the Au substrates was estimated by comparing the weight of a paper photocopy to that of a 1 cm^2 of paper.

Hybridization of ssDNA-Au. The purified ssDNA-Au NP product was stored in the 0.01% SDS, with the latter being removed immediately prior to use, as described below. The ssDNA-Au NPs were centrifuged at 14800 rpm for 15 min at 15 °C, the supernatant removed, and the pellet resuspended in the hybridization buffer,

(7) Grabar, K. C.; Freeman, R. G.; Hommer, M. B.; Natan, M. J. *Anal. Chem.* **1995**, *67*, 735.
(8) Taton, T. A. *Curr. Protocol. Nucl. Acid Chem.* 2002, Unit 12.2.
(9) Hurst, S. J.; Lytton-Jean, A. K. R.; Mirkin, C. A. *Anal. Chem.* **2006**, *78*, 8313.
(10) Keating, C. D.; Kovaleski, K. M.; Natan, M. J. *J. Phys. Chem. B* **1998**, *102*, 9404.

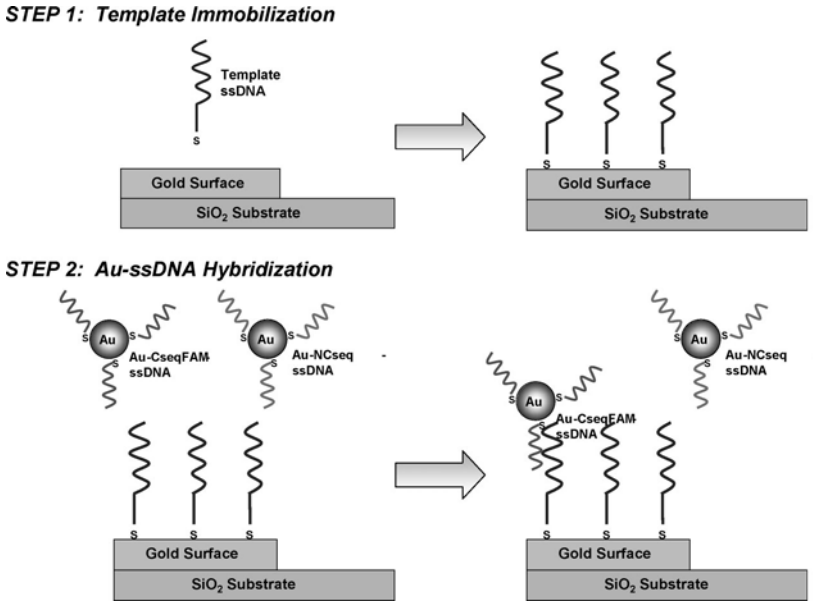

Figure 1. Schematic of basic reactions studied.

such that the Au NPs were diluted by a factor of 2, yielding a final concentration of ~15 nM. The SiO_2/Au electrode substrates, exposed to the ssDNA template for a minimum of 12 h, were then rinsed thoroughly in MilliQ water, and dried with nitrogen. The substrates were placed in a clean plastic Petri dish containing damp Kimwipes and 25 μL of the Au-ssDNA sample in hybridization buffer pipetted onto the surface of the substrate. The lid was then placed onto the Petri dish, and the dish covered with the damp Kimwipes so as to generate a humid environment and prevent evaporation of the Au-ssDNA sample solution from the surface. The substrates were typically incubated overnight (12−14 h) at RT, before they were removed from the Petri dish, extensively washed with MilliQ water, and dried with nitrogen. The resulting substrate surface was then characterized using SEM (see details below). The optimal hybridization buffer for this study was found to be 25 mM PB (pH 7.2) + 2 M NaCl + 0.05% Tween 20, however a variety of conditions, including NaCl concentration, exposure time and exposure temperature, were investigated as detailed in the Results and Discussion section.

SEM Characterization and Image Analysis. As is evident from the images shown in this paper, the 12 nm Au NPs are quite easily seen using the in-line detector of the SEM (Carl Zeiss SMT Supra 55; Carl Zeiss SMT, Inc., Peabody, MA) at 5kV on either SiO_2 surfaces or on evaporated Au surfaces. The latter is particularly noteworthy given the lack of contrast (i.e., Au on Au) and the roughness of the evaporated Au surface. For assessing the Au NP coverage on a given sample, SEM images were taken at magnifications of 100k× and 200k×; the former gave a qualitative assessment while the latter, generally focused only on the Au surfaces, and was used for quantitative evaluation. Since there is dispersion in Au NP size, for convenience we gauged the "Au NP coverage" by the percent of projected (rather than true) area of the surface that is covered by Au NPs as seen in SEM. These area estimates were obtained from the SEM images using Digital Micrograph Software from Gatan, Inc. In order to evaluate errors, five portions of each full 200k× image were examined separately, and the values and error bars were then estimated from this information. Generally speaking, the errors are reasonably small as will be seen below.

Results and Disscusion

Initial Optimization Studies. Figure 1 illustrates the main objective of this study, namely, to utilize the hybridization reaction between complementary strands of ssDNA to selectively functionalize micron-sized gold features patterned on SiO_2 surfaces. Optimization required studying the conditions for ssDNA attachment to both the Au NPs and the gold surfaces, and then their subsequent hybridization.

As mentioned earlier, for use in this study Au NPs coated with ssDNA were prepared according to optimized protocols published by Hurst and co-workers.[9] These Au NPs were functionalized with thiol-terminated 15mer ssDNA, either complementary or noncomplementary to the ssDNA template sequence immobilized on the gold modified substrates. The UV−visible absorption of purified NPs modified either with NCseq, Cseq or CseqFAM, showed a surface plasmon (SP) shift of 2−3 nm relative to the unmodified NPs, evidence of a change in the local refractive index in the immediate vicinity of the NP surface that is associated with the ssDNA modification (see Supporting Information). A DTT displacement assay using Au NPs modified with fluorescently labeled ssDNA (CseqFAM) indicates that, for a starting ratio of 1:300 Au/ssDNA, there are roughly 75 ssDNAs on each Au NP (see Supporting Information).[9] Hurst and co-workers found similar ratios, albeit using slightly larger 15 nm Au NPs functionalized with 25mer ssDNAs that included a 10 mer poly "A" spacer.[9]

A first area of optimization in this study was in the functionalization of the micron-sized gold features of the SiO_2/Au substrates with the thiol-terminated ssDNA template. For these experiments we used the 25mer ssDNA template (see Table 1) containing a 10mer poly "T" spacer to distance the sequence-specific portion of the DNA from the gold surface. The poly "T" spacers were chosen on the basis of literature studies that demonstrate its weaker relative affinity for gold surfaces as compared to the other nucleotides.[11,12] In preliminary experiments the ssDNA 25mer template was exposed to the SiO_2/Au substrates in MilliQ water. Following a subsequent exposure to Cseq-Au (complementary) or NCseq-Au (noncomplementary) NPs, SEM images of the surface revealed that both ssDNA-Au NPs bound equally well to the gold features of the substrates (data not shown), suggesting a high degree of nonspecific binding. Similar observations were made on unmodified SiO_2/Au substrates

(11) Demers, L. M.; Ostblom, M.; Zhang, H.; Jang, N. H.; Liedberg, B.; Mirkin, C. A. *J. Am. Chem. Soc.* **2002**, *124*, 11248.
(12) Kimura-Suda, H.; Petrovykh, D. Y.; Tarlov, M. J.; Whitman, L. J. *J. Am. Chem. Soc.* **2003**, *125*, 9014.

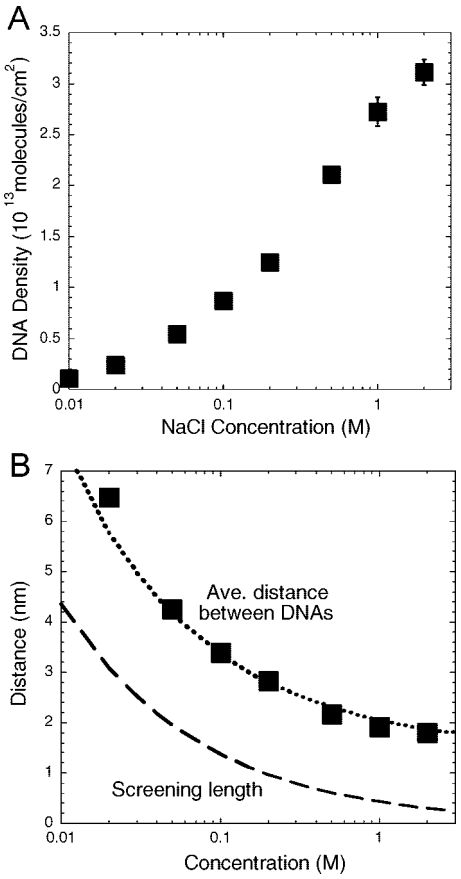

Figure 2. DNA template density. (A) Surface density (per unit projected area) of DNA on Au electrode surface as a function of NaCl concentration as determined by DTT assay. (B) Average distance between DNAs on the surface as estimated from the surface density. Also shown is the screening length (dashed curve) and a curve-fit to the data (dotted curve) based on assuming a proportionality to the screening length with an additive minimum (1.4 nm) set by steric effects.

exposed to the ssDNA-Au NPs, while plain Au NPs did not bind. Together these results suggest that when MilliQ water was used as the immobilization buffer, very little template was bound to the Au surface. They also suggest (since the unmodified Au NPs did not bind) that it is the ssDNA on the NP surface that mediates the observed nonspecific binding to the gold surface. This observation is not surprising given the known affinity of DNA for gold surfaces, but does not explain the lack of template on the gold surface.[12]

Hypothesizing that the apparent low template coverage was due to the highly charged nature of DNA, we investigated increasing the NaCl concentration in the immobilization buffer to raise the surface density of the ssDNA template. For this study we used the Fluor25mer and Au substrates and the surface DTT assay as described in the experimental section. From this the ssDNA template surface density as a function of NaCl concentration can be calculated as shown in Figure 2A. Clearly, even the addition of 0.1 M NaCl is sufficient to increase the concentration of Fluor25mer template immobilized on the Au surface greatly, in agreement with studies by a number of groups.[13,14] An alternative version of Figure 2A is shown in Figure 2B with the data converted into an average distance between surface-bound DNAs. That the observed behavior is

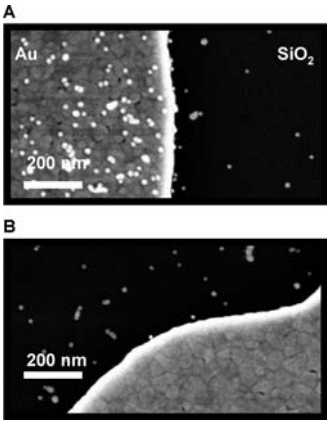

Figure 3. Template-Au surface optimization. SEM images of gold features on silicon substrates modified with 2 μM 25mer ssDNA template (deprotected prior to use) in 1xTE + 2 M NaCl + 0.05% Tween 20 at RT overnight then exposed to 15 nM Au NPs modified with either (A) complementary, Cseq, or (B) noncomplementary, NCseq, ssDNA (in 25 mM PB + 0.05% Tween 20 + 0.5 M NaCl).

due to the electrostatic screening effect of the NaCl (that allows for greater template packing on the Au substrate surface) is suggested by the fact that the data is seen to track the calculated screening length versus the NaCl concentration quite closely.[13,14] This is demonstrated quantitatively by the dotted line through the data that is the result of a simple curve-fit based on assuming the distance is proportional to the screening length with some additive minimum (1.4 nm) set by steric effects. Based on this data, most of the remaining experiments of this paper utilize 2 M NaCl for the template depositions in order to ensure a maximal density of available templates.

Following the protocol described above for template immobilization, SiO_2/Au substrates were functionalized with 25mer template in 1xTE + 2 M NaCl + 0.05% Tween 20. The modified substrates were then exposed to Cseq-Au (complementary) or NCseq-Au (noncomplementary) NPs with the resulting SEM images shown in panels A and B of Figure 3, respectively. Clearly, binding of the ssDNA-Au NPs is observed only for the complementary Au NPs on the gold regions of the substrate (lighter portion of the SEM image), thereby illustrating the specific nature of the DNA hybridization. Some nonspecific binding is seen on the SiO_2 regions (darker portion of the SEM image) but it is minimal in comparison to the gold, thus clearly demonstrating that DNA hybridization can be used to specifically immobilize ssDNA-Au NPs onto the gold features present on a mixed SiO_2/Au substrate.

With the selective attachment of Au NPs to Au electrodes by DNA hybridization demonstrated, we next attempted to optimize this process, with the optimum being defined as having as dense an NP coating on the Au electrodes as possible, while retaining high selectivity against noncomplementary Au NPs and against nonspecific deposition on the SiO_2 surface. A number of variables that could potentially affect the deposition were investigated, including the NaCl concentration, the surface density of DNA templates, the ssDNA-Au NP concentration, the hybridization time, and the hybridization temperature. In the figures to follow we show only SEM images of the gold electrode portions of the SiO_2/Au substrates following their exposure to Cseq-Au (complementary) NPs. In all cases, equivalent experiments with NCseq-Au (noncomplementary) NPs showed essentially no binding whatsoever to either the Au or the SiO_2 portions of the substrate (data not shown). Moreover, nonspecific binding to the SiO_2 portion by the Cseq-Au NPs was minimal when the Tween 20

(13) Petrovykh, D. Y.; Kimura-Suda, H.; Whitman, L. J.; Tarlov, M. J. J. *Am. Chem. Soc.* **2003**, *17*, 5219.
(14) Huang, E.; Satjapipat, M.; Han, S. B.; Zhou, F. M. *Langmuir* **2001**, *17*, 1215.

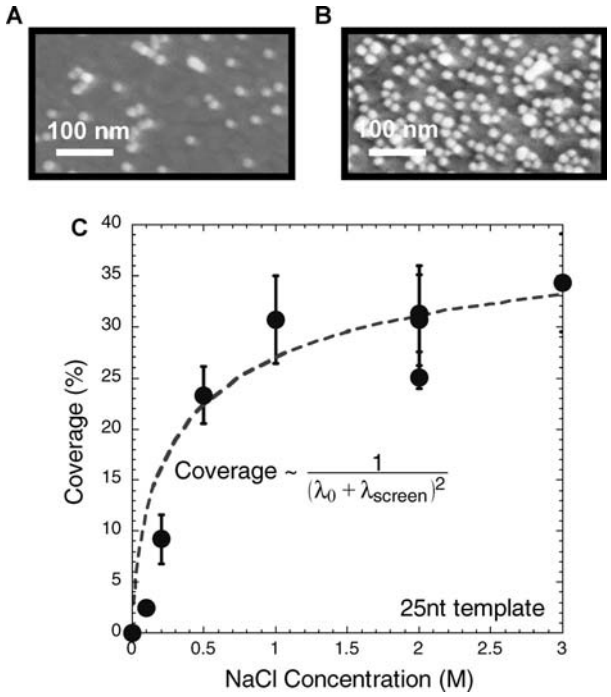

Figure 4. Hybridization optimization−NaCl concentration. SEM images of 15 nM Cseq-Au NPs exposed to 25mer ssDNA template modified surfaces in the presence of 25 mM PB pH 7.2 plus either (A) 0.2 M or (B) 2.0 M NaCl at RT overnight. (C) A graph of the real NP coverage (in %), determined from the SEM images, as a function of the NaCl concentration present in the hybridization buffer. The curve is a fit to the coverage based on assuming it varies inversely as a function of the screening length as shown.

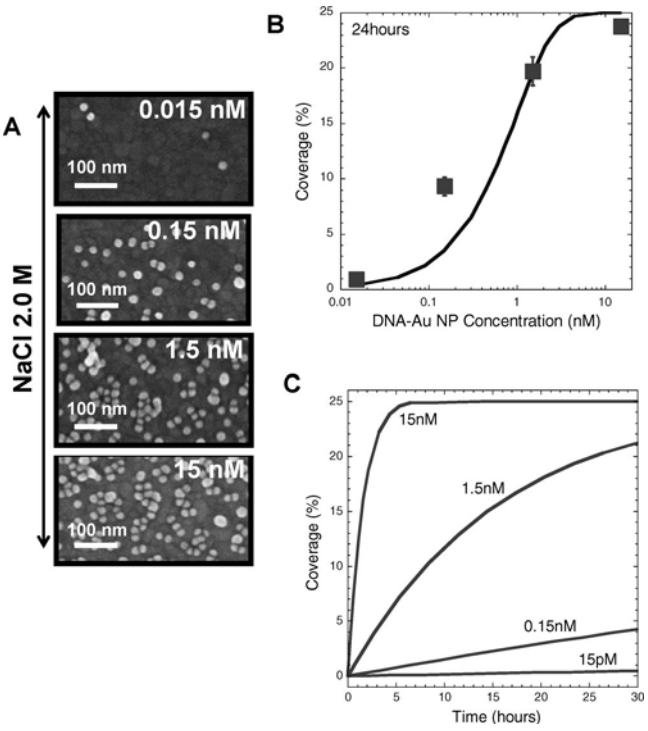

Figure 5. Hybridization optimization−Cseq-Au NP concentration. (A) SEM images of 25mer ssDNA template modified substrates exposed to Cseq-Au NPs (in 25 mM PB + 0.05% Tween 20 + 2.0 M NaCl) at (i) 0.015 nM, (ii) 0.15 nM, (iii) 1.5 nM and (iv) 15 nM. (B) Graph illustrating the Au NP coverage (in %), determined from the SEM images, as a function of the Cseq-Au NP concentration. The error bars indicate plus/minus two standard deviations. (C) Simulation of the % Coverage as a function of time and concentration.

surfactant was used; if the surfactant was not present or when an alternative surfactant SDS was employed, nonspecific binding was augmented.

Varying the concentration of the NaCl in the hybridization buffer over the range from 0 to 3 M was found to affect the Au NP coverage significantly. Some illustrative SEM images are displayed in Figure 4. The images in Figure 4A and 4B show the Au portion of SiO_2/Au substrates exposed to Cseq-Au NPs in the presence of 0.2 and 2.0 M NaCl, respectively. Clearly, the higher NaCl concentration yields an improved surface coverage. A summary plot of the measured Au NP coverage (circles), as a function of the NaCl concentration in the hybridization buffer, is shown in Figure 4C. The line in the figure is a curve-fit based on the assumption that the Au NP coverage varied inversely as the square of the screening length as discussed further below. Because Figure 4C shows only incremental increases in % coverage at the highest hybridization buffer concentrations, we did not study concentrations greater than 3 M NaCl. We also observed that the Tween 20 surfactant used to block nonspecific binding to the SiO_2 improved the coverage of the Cseq-Au NPs by 2−3% on the gold electrodes (data not shown). Finally, the addition of di- and trivalent cations, such as Mg^{2+}, Ca^{2+}, Ba^{2+} and Al^{3+}, was investigated as a possible means of enhancing the screening of the ssDNA-Au NP charge. Unfortunately, even when these ions were at the low concentration of 0.1 M, both the purified Cseq-Au NPs and NCseq-Au NPs were found to aggregate (data not shown).

A second test of the hybridization of Cseq-Au NPs with cDNA templates bound to Au electrodes was to examine the effect of the Cseq-Au NPs concentration over the range from 0.015 to 15 nM while keeping the NaCl concentration fixed at 2 M. As seen in Figure 5A, after 12 h exposure the maximum coverage of ~25% was reached when the NP concentration was 15 nM. Below this value the coverage after 12 h increased roughly logarithmically in the concentration. The lines in Figure 5B and C were obtained using numerical simulation as discussed below in connection with Figure 7.

To further understand the hybridization of Cseq-Au NPs (at 15 nM in 25 mM PB + 2 M NaCl + 0.05% Tween 20) with the cDNA templates on Au electrodes, we studied the effect of hybridization time and temperature. The time study is illustrated in Figure 6 with Figure 6A showing SEM images of the Au electrodes after 10 min (i), 1 h (ii) and 14 h (iii) with the latter obviously yielding a far denser coverage. The entire data set is summarized in Figure 6B where we show the measured Au NP coverage versus the square root of time, with data taken from two separate experiments, and at three different temperatures ranging from room temperature (~24 °C) to 60 °C. Note that 60 °C is above the melting temperature of the 25mer template (52.9 °C), but the substrates were allowed to cool for 2−3min prior to being rinsed. It is apparent that while at 60 °C a plateau is reached quicker than at 37 °C or RT, all temperatures yield approximately the same plateau with a Au NP coverage of ~25%. The lines in Figure 6B are modeling results obtained by the same methods used in Figure 5B and C, and that are discussed next.

Modeling and Simulation. As an aid to understanding the concentration, time and temperature dependences of Figures 4C, 5B and 6B, we performed numerical simulations based on a simple one-dimensional continuous reaction-diffusion model that is similar to that reported by Axelrod and co-workers.[15] The governing differential equation is the diffusion equation with the diffusion constant D of the 12 nm particles assumed to take the Stokes−Einstein value of about 4×10^{-11} cm^2/s at room temperature. (A more sophisticated model in which the excluded

volume was taken into account was also considered, but as this refinement seemed to have little effect on the results, it is not discussed further here.) The initial condition is that the Au NP concentration $C = C_0$ where C_0 is the Au NP concentration in solution at $t = 0$, and we assume the solution volume large enough that it can be taken to be semi-infinite so that this same condition can be applied at all times at positions far from the substrate. To derive the critical boundary condition at the electrode surface (at $x = 0$), we assume a simple reaction of

$$\text{Templated gold electrode} + \text{DNA-NP(free)} \rightleftarrows \text{NP(bound)} \quad (1)$$

Taking S to the density (per unit area) of NPs hybridized to the surface, M to be the maximum possible NP density on the surface and $U = M - S$, first-order reaction kinetics then gives the boundary condition:

$$\frac{\partial S}{\partial t} = D\left(\frac{\partial C}{\partial x}\right)_{x=0} + k_F C U - k_R S \quad (2)$$

where k_F and k_R are the rate constants for the forward and reverse reactions. At long times, these kinetics obviously approach the Langmuir isotherm with

$$\text{Equilibrium Coverage} = \left(\frac{S}{M}\right)_{t\to\infty} = \frac{\alpha C_0}{1+\alpha C_0} \text{ where } \alpha \equiv \frac{k_F}{k_R} \quad (3)$$

To use the foregoing theory to help understand the experiments, we first fit the room temperature data of Figure 6B using the following procedure. Knowing the concentration C_0 and the measured equilibrium coverage of 25% we can use the Langmuir isotherm to determine α to be 1.1×10^{-14} cm^3. Then we simulate numerically the transient and curve-fit the room temperature data of Figure 6B utilizing k_F as the fitting parameter. The value so determined, $k_F = 8.3 \times 10^4$ cm^3/s, yields the excellent fit shown in Figure 6B (24C curve). The quality of the fit and the reasonableness of the model and parameters lead us to believe that first-order kinetics provides an accurate representation of the physics/chemistry of ssDNA-Au NP-template hybridization at the surface. To obtain good fits for the temperature behavior (also shown in Figure 6B) we further assume, as seems realistic, that the reaction kinetics is temperature-activated with an activation energy of 0.8 eV. Finally, in Figure 5C we show the equivalent of Figure 6B but with predictions for various other values of C_0. The lower concentration values of Figure 5B are clearly kinetically limited over the time simulated. The particular values at 24 h from Figure 5C (as well as many other similar simulations) are plotted as the line in Figure 5B. As seen in the figure, these predictions are in fair agreement with the experimental values also shown in that plot. The observed discrepancies between simulation and experiment could easily arise from the simplified nature of our model, however, it is worth noting that relatively small changes in concentration (e.g., due to evaporation during the experiment) and/or temperature could also be responsible.

Improving Au NP Surface Coverage. The one remaining puzzle in Figures 4, 5, and 6 is why the maximum total coverage seems invariably limited to about 35%. This was observed in all of our experiments over several different lots of Au NPs, DNA purchases, and substrates. Possible explanations could relate to the templates, the ssDNA-Au NPs or the substrates. The fact that, as seen in Figure 4C, increasing NaCl concentration during hybridization leads to greater coverage (up to 35% when the NaCl concentration is 3 M) immediately suggests a role for electrostatic repulsion and screening. But how this mechanism can explain the unexpectedly small asymptote is unclear.

To explore this question further we carried out several additional experiments. The first measured the hybridization yield of target DNA to surface-bound templates when the former were *not* attached to NPs. This yield was monitored by tagging the target DNA with a fluorophore and using the DTT assay. And in reasonable agreement with the literature,[17] the result (data not shown) is that the hybridization yield is quite low being less than 1% under the relevant conditions. This suggests that a lack of *availability* of template (presumably due to its lying "flat" on the Au surface) could be responsible for our reduced NP coverage. However, this conclusion is at odds with four other lines of evidence:

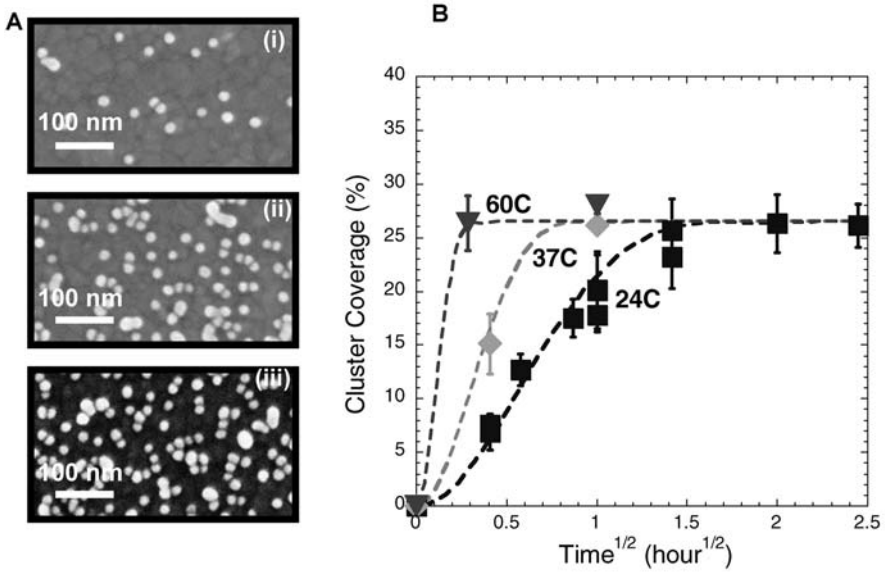

Figure 6. Hybridization optimization−time and temperature study. (A) SEM images of 25mer ssDNA template modified substrates exposed to 15 nM Cseq-Au NPs (in 25 mM PB + 0.05% Tween 20 + 2.0 M NaCl) for (i) 10 min, (ii) 1 h, and (iii) 14 h. (B) Graph illustrating the Au NP coverage (in %), determined from the SEM images, as a function of the $\sqrt{}$time for three different temperatures (points) and the numerical curvefits (lines) to these data as discussed in the text. The error bars indicate plus/minus two standard deviations.

(i) As discussed by Peterson and co-workers[17] (and confirmed as part of our measurements described in the previous paragraph), in the absence of NPs a higher density of template DNAs actually reduces the number of ssDNAs that will hybridize, presumably due to steric effects. But when the same experiment is performed with ssDNA-Au NPs (again by controlling the template density using the NaCl concentration according to Figure 2A) we find (data not shown) that the highest NP coverage instead occurs when the template density is greatest.

(ii) A well-known method[18] for increasing the availability of surface-bound template DNAs for hybridization with target ssDNAs is to follow the deposition of the template DNA with a "backfill" step in which the surface is exposed to mercapto-hexanol (MCH). However, when we utilized this technique, we found that when the backfilled surface was exposed to Cseq-Au NPs, the backfilling actually caused the NP coverage to be reduced, again suggesting that the availability of template was not the limiting factor.

(iii) Another way of affecting the availability of surface-bound DNA to target DNA is to introduce various spacer groups aimed at increasing the distance between the template DNA and the surface (presuming that the template DNA is attached by its thiol which may not be true). One such approach, motivated by the work of Kimura-Suda and co-workers,[12] is to use a length of poly "T" as the spacer, while another commonly used method involves a PEG spacer. When the poly "T" method was tested for its effectiveness in enhancing the hybridization of Cseq-Au NPs, we found very little effect as the length of spacer varied from zero to 20 "T"s in length. The SEM images for hybridization of Cseq-Au NPs after 14 h are shown in Figure 7 with the poly 10 (Figure 7B) and poly 20 "T" (Figure 7C) spacers giving similar coverages of 25−30%, while having no spacer (Figure 7A) gave only a slightly lower coverage of 20−25%. Curiously, when the PEG spacer was used (Figure 7D), the coverage dropped to only 5% for unknown reasons.

(iv) Finally, from a quantitative perspective, our measurements of the active templates when no NP was present found the density to be so low that, if this were to determine the NP density, the maximum coverage would be below 10%, rather than the measured 25−35%.

On the basis of these observations we conclude that the process of hybridization to surface-bound DNA templates must be different when the target DNA is free versus when it is bound to a NP. As to why this might be, we can speculate that in the NP case having multiple cDNAs in close proximity may well lead to cooperative effects that enhance the hybridization yield. Alternatively, it could be the increased residence time of the cDNA when it is attached to a NP that is critical in enhancing the hybridization yield. To understand better either of these mechanisms would require detailed microscopic modeling and is therefore beyond the scope of this work. Such modeling would not only need to understand the simultaneous interaction of multiple cDNAs with surface-bound DNAs, but as shown by the effect of salt (Figure 4C) it would likely also have to take into account strong hydration forces that would arise from the DNA's hydrophilic nature.[16] In addition, such an analysis would have to comprehend the effect of surface roughness. That the latter is important is shown by hybridization experiments performed by us on "flat" Au surfaces (created by evaporation on mica) where the resulting NP depositions were found to be greatly reduced (data not shown).

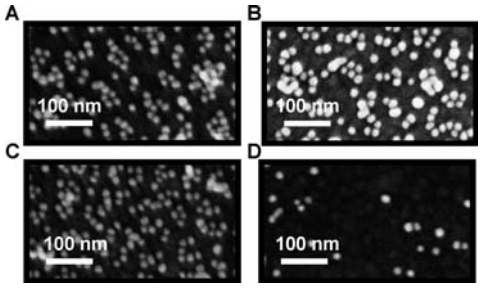

Figure 7. Template spacer study. SEM images of hybridization studies between 15 nM Cseq-Au NPs (in 25 mM PB + 0.05% Tween 20 + 2.0 M NaCl) and substrates functionalized with templates (A) 15mer−zero spacer, (B) 25mer−10 poly "T" spacer, (C) 35mer−20 poly "T" spacer and (D) Peg-15mer−iSp9 spacer.

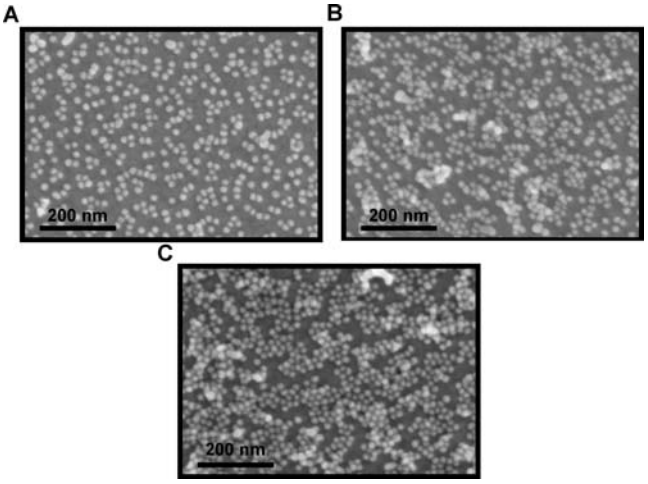

Figure 8. Multilayer study. SEM images of 25mer ssDNA template modified substrates exposed to (A) Cseq-Au NPs−1 layer, (B) Cseq-Au NPs then NCseq-Au NPs−2 layers and (C) Cseq-Au NPs then NCseq-Au NPs then Cseq-Au NPs−3 layers. Note all NPs were 15 nM in 25 mM PB + 0.05% Tween 20 + 2.0 M NaCl with extensive MilliQ water washing steps between layers.

Ideally for electronic applications a higher surface coverage of the Au NPs would be desirable. In an attempt to further increase the surface coverage we investigated the use of multilayers of ssDNA-NPs using NPs functionalized with Cseq and NCseq 15mer ssDNA that are complementary to each other. For this experiment, SiO_2/Au substrates were sequentially exposed to Cseq-Au NPs, to NCseq-Au NPs, and then again to Cseq-Au NPs. The resulting SEM images taken at various stages of the modification are displayed in Figure 8. As observed previously, the first exposure to Cseq-Au NPs resulting in an 25−30% coverage of the Au NPs, this increased to ∼45% upon exposure to NCseq-Au NPs (2nd layer Au NPs) and then further to ∼60% following the second Cseq-Au NPs exposure (3rd layer Au NPs). Clearly, multiple deposition cycles can be used as a method to increase the surface density of the Au NPs on Au surfaces.

Conclusion

Motivated by the technological promise of gold nanoparticles (Au NPs) for electronics and sensors, we investigated in a systematic manner the selective assembly of such NPs on

(15) Axelrod, D.; M.D., Wang *Biophys. J.* **1994**, *66*, 588.
(16) Israelachvili, J., *Intermolecular & Surface Forces*, 2nd ed.; Academic Press: London, 1991; p 276.
(17) Peterson, A. W.; Heaton, R. J.; Georgiadis, R. M. *Nucleic Acids Res.* **2001**, *29*, 5163.
(18) Herne, T. M.; M.J., Tarlov *J. Am. Chem. Soc.* **1997**, *119*, 8916.

electrodes via DNA hybridization. Protocols are reported that maximize the selectivity and coverage when 15mers are used as the active binding agents. Detailed studies of the dependences on time, ionic strength, and temperature reveal the underlying mechanisms and their limits. Under optimized conditions, coverage of Au NPs on Au electrodes patterned on silicon dioxide (SiO_2) substrates was ~25−35%. In all cases, Au NPs functionalized with non-complementary DNA showed negligible attachment and nonspecific adsorption on the SiO_2 surfaces of the patterned substrates was essentially absent. The DNA-guided assembly of multilayers of NPs was also demonstrated and, as expected, was found to further increase the coverage, with three deposition cycles yielding a surface coverage of approximately 60%.

Acknowledgment. The authors thank Drs. A. W. Snow and J. Rife for helpful discussions and the Office of Naval Research for funding support.

Supporting Information Available: Details regarding the synthesis, purification and characterization of the ssDNA-Au-NPs. This material is available free of charge via the Internet at http://pubs.acs.org.

LA800640U